

A fast algorithm for material image sequential stitching

Boyuan Ma^{a,b,c}, Xiaojuan Ban^{a,b,c,*}, Haiyou Huang^{a,d,e,*}, Wanbo Liu^{a,d}, Chuni Liu^{a,b,c}, Di Wu^f, Yonghong Zhi^g



^a Beijing Advanced Innovation Center for Materials Genome Engineering, Xueyuan Road 30, Haidian District, Beijing 100083, China

^b School of Computer and Communication Engineering, University of Science and Technology Beijing, Xueyuan Road 30, Haidian District, Beijing 100083, China

^c Beijing Key Laboratory of Knowledge Engineering for Materials Science, Xueyuan Road 30, Haidian District, Beijing 100083, China

^d Institute for Advanced Materials and Technology, University of Science and Technology Beijing, Xueyuan Road 30, Haidian District, Beijing 100083

^e Key Laboratory of Environmental Fracture (Ministry of Education), University of Science and Technology Beijing, Xueyuan Road 30, Haidian District, Beijing 100083, China

^f Department of ICT and Natural Sciences, Norwegian University of Science and Technology, Aalesund, Norway

^g Mechanical and Electrical Design and Research Institute of Shanxi Province, Shengli Street 228, Xinghualing District, Taiyuan City, Shanxi Province 030009, China

ARTICLE INFO

Keywords:

Micrograph stitching
Feature matching
GPU acceleration

ABSTRACT

In material research, it is often highly desirable to observe images of whole microscopic sections with high resolution. So that micrograph stitching is an important technology to produce a panorama or larger image by combining multiple images with overlapping areas, while retaining microscopic resolution. However, due to high complexity and variety of microstructure, most traditional methods could not balance speed and accuracy of stitching strategy. To overcome this problem, we develop a method named very fast sequential micrograph stitching (VFSMS), which employ incremental searching strategy and GPU acceleration to guarantee the accuracy and the speed of stitching results. Experimental results demonstrate that the VFSMS achieve state-of-art performance on three types' microscopic datasets on both accuracy and speed aspects. Besides, it significantly outperforms the most famous and commonly used software, such as ImageJ, Photoshop and Autostitch. The software is available at https://www.mgedata.cn/app_entrance/microscope.

1. Introduction

Microstructure is the classic term used in metallography to describe small scale structure features in the scale less than 1000 μm [1]. The microstructure of a material (such as metals, ceramics, polymers or composites) can strongly influence almost all properties such as mechanical properties, physical properties, corrosion resistance, etc., which govern the application of the material in industrial practice. The microstructure is often observed and analyzed using various microscopy methods such as optical microscopy, electron microscopy, etc. according to the necessary of examining and determining magnifications [2,3]. With the development of material design, integrated design from micro- or nano-structure of materials to large-scale structure of components has aroused more and more attention from material scientists and engineers. Multi-scale material design often need illustrate macro- and micro-structure simultaneous. A large-scale panorama of material or component with micro-level resolution may help multi-scale and integrated design of material and component. Fig. 1 shows a sample of a large-scale panorama (35 mm × 17 mm) of a cross section for Ni-

based superalloy turbine blade with a high resolution (10 μm) obtained by Prof. Feng's group to assist the optimization of service performance.

However, due to the limitation of imaging principle, it is usually difficult to get a single image with high resolution to view a whole sample with large size [4]. A usual solution is to stitch several local images with overlapping areas to form a global composite one, which refers to as *Stitching* [5,6]. Some examples of optical micrograph stitching in material researches are shown in Fig. 2. We demonstrate three types' microscopic images with different shooting paths, which represented by red dashed line. Besides, the red translucent regions refer to a shot of microscope. As shown in the figure, there are some challenges in the stitching processes: First, the micrographs have high complexity and compose of diverse tiny microstructures, which increases demand for robustness of stitching strategy. Second, microscopic images usually have high resolution which increases demand for efficiencies of stitching strategy. Third, there is no static shooting path in actual practice, so the stitching strategy should self-adaptive to any situation.

Currently, many stitching methods and software can be categorized into two classes: Feature based and Phase correlation based [7].

* Corresponding authors at: Beijing Advanced Innovation Center for Materials Genome Engineering, Xueyuan Road 30, Haidian District, Beijing 100083, China.
E-mail addresses: banxj@ustb.edu.cn (X. Ban), huanghy@mater.ustb.edu.cn (H. Huang).

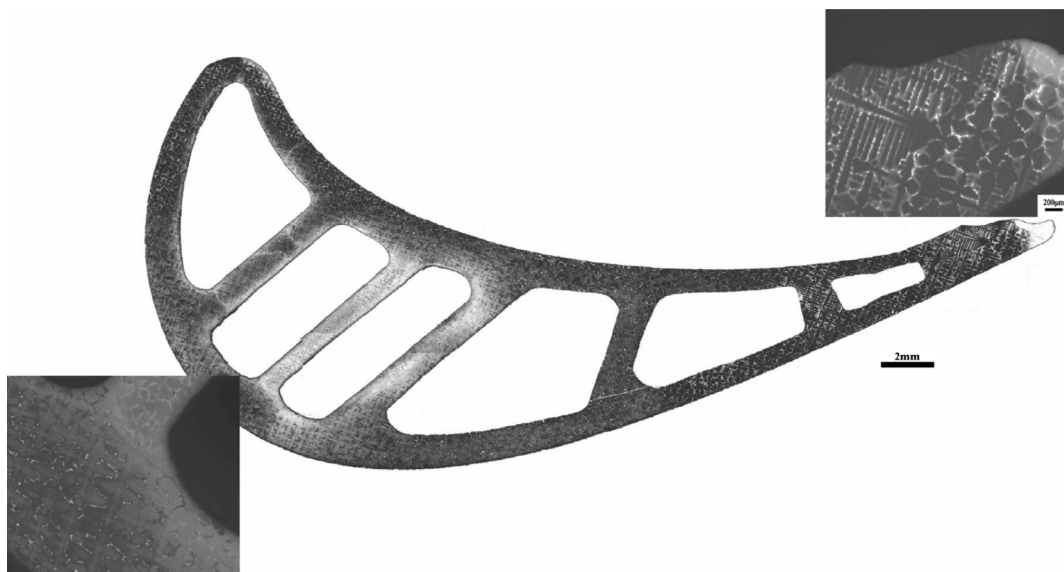


Fig. 1. a large-scale panorama ($35\text{ mm} \times 17\text{ mm}$) of a cross section for Ni-based superalloy turbine blade with a high resolution ($10\text{ }\mu\text{m}$) for multi-scale and integrated design of material and component.

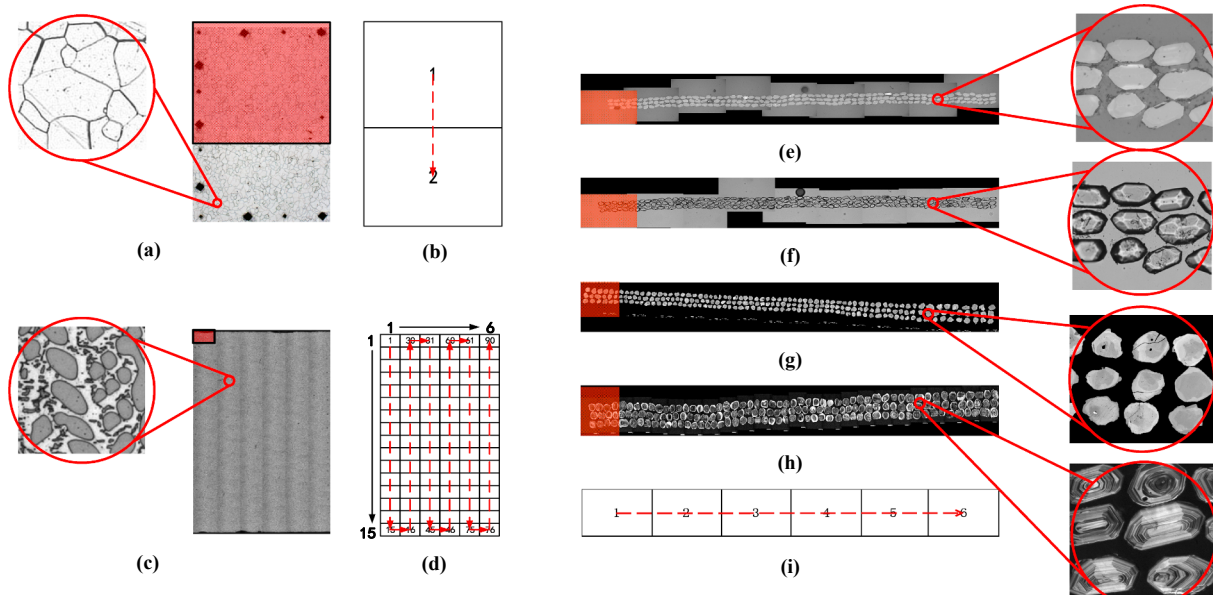


Fig. 2. Three types' local and global micrographs and their shooting path. The red translucent regions represent one shot from microscope. The red dashed lines refer to the shooting path. (a) Optical microscopy (OM) image of Iron polycrystal with its detail imaging. (b) Pairwise shooting path of (a) with 2 local images. (c) OM image of dendritic crystal with its detail imaging. (d) Grid shooting path of (c) with 90 local images. (e) Scanning electron micrographs of zircon in reflected mode (SEM-RE), (f) in transmission mode (SEM-TR), (g) in black scattered mode (SEM-BS), and (h) cathodoluminescence mode (SEM-CL) respectively with its detail imaging. (i) Shooting path for (e)–(h), the number of local images depends on the length of sample. (For interpretation of the references to color in this figure legend, the reader is referred to the web version of this article.)

Feature based stitching methods can achieve high accuracy with invariant features, such as SIFT [8,9], SURF [10,11] and ORB [12]. These methods establish correspondences between points, lines, edges, corners, or other geometric entities. Characteristics of robust detectors include invariance to image noise, scale invariance, translation invariance, and rotation transformations. However, since the microstructures are always highly complicated, most of these methods can extract thousands of features to match, which may cause time consumption and a heavy computational burden so that couldn't be applied in real time [13,14]. Some works try to sample the image in order to decrease the time consumption of feature searching and matching [6,18]. However, these methods will unavoidably lose the information in micrograph. Besides, most of them apply ransac [15] and

homography [16,17] to match two sequential micrographs, which are suited for nature scene and will cause some deformations for local micrographs in horizontal translation model.

Phase correlation based methods can achieve real time stitching by using implementation of fast fourier transformation (FFT) [19,20]. Most software build upon those methods by considering the speed demand of users [21,24,25]. However those may yield ambiguous results when micrographs contain much of similar microstructures [26], which will lead low accuracy when stitching.

In this work, we describe a developed stitching method, named very fast sequential micrograph stitching (VFSMS), to balance the accuracy and speed of stitching strategy. Our algorithm presents three contributions:

- (1) Incremental searching strategy and corresponding matching and fusing method. Those make the algorithm achieve improvement both on accuracy and speed aspects.
- (2) GPU acceleration. We introduce GPU acceleration in feature search process which make stitching could be applied in real time, even for the complicated micrograph with huge resolution. It is the first demonstration of GPU acceleration in this context that in particular has substantial gains in the aspects of stitching speed.
- (3) Sequential stitching. The algorithm developed in this paper is completely automated for fast stitching of micrographs. There is no need to design the shooting path.

Experimental results demonstrate that VFSMS achieves state-of-art performance on several microscopic datasets on both accuracy and speed aspects. Besides, it significantly outperforms the most famous and commonly used software, such as ImageJ [21,27], Photoshop [24] and Autostitch [28,29]. The average time consumption of VFSMS is 60% of ImageJ, which is most popular software in material image processing. In addition, VFSMS achieves 100% accuracy in experimental datasets, which is more robust than other software.

The remainder of this paper is organized as follows: In Section 2, we provide a description of the VFSMS. In Section 3, we present experiments on different stitching methods to show the effectiveness and efficiencies of the proposed approach. Besides, we discuss the results of different methods in Section 4. Finally, we conclude the paper in Section 5.

2. Method

2.1. Framework of the VFSMS

VFSMS is a feature based image stitching method. For traditional feature based method, it is used to extract thousands of features in one local image, which may cause time consumption and a heavy computational burden so that cannot be applied in real time [13,14]. In order to handle this problem, we proposed to use incremental searching strategy and GPU acceleration to increase stitching speed and robustness.

The flowchart of VFSMS is shown in Fig. 3. First, we input micrograph sequences, the algorithm will carry on if there is any micrograph never been calculated. Second, it uses incremental searching strategy to find pairs of feature points and match them. The detailed flowchart and diagram of incremental search can be found in the Section 2.2. The detailed match method could be found in the Section 2.3. If the last two sequential micrographs match correct, the algorithm will record the

offset (between original point of next image and that of last image) and stitch next micrograph. Otherwise the algorithm will interrupt the stitch and restart from next micrograph if not correct. Therefore, VFSMS will save stitch previous results and restart the stitch on the next images when it faces mismatch, which is designed for multi section stitch. Third, it uses trigonometric function to fuse images and eliminate obvious seamline. The detailed of fusing algorithm can be found in the Section 2.4. Finally, it gets stitching output result.

2.2. Incremental searching strategy

We demonstrate the schematic diagram and flowchart of incremental searching strategy in Figs. 4 and 5. Let $f_1(x, y)$ and $f_2(x, y)$ represent the two sequential local micrographs. There are three parameters influence the algorithm's performance: local direction, incremental parameter and feature search length. Local direction means stitching direction of two sequential micrographs. As shown in the Fig. 4, when it equals 0, it means the first image locates at the above of the second image. 1 means the first image locates at the left of the second image. 2 means the first image locates at the bottom of the second image. And 3 means the first image locates at the right of the second image. Incremental parameter is constrained to be any of -1, 0 or 1, which control stitching direction in the next stage. For example, let $local\ direction_{previous}$ represents the previous local stitching direction of the first and the second micrographs and $local\ direction_{next}$ represents the next local stitching direction of the second and the third micrographs. If incremental parameter equals 0, the $local\ direction_{next}$ is consistent with $local\ direction_{previous}$. If incremental parameter equals 1, the algorithm will turn $local\ direction_{previous}$ 90 degrees clockwise to form $local\ direction_{next}$. If incremental parameter equals -1, the algorithm will turn $local\ direction_{previous}$ counterclockwise 90 degrees to form $local\ direction_{next}$. The algorithm uses following Eq. (1) to update the local direction when the algorithm cannot find correct result in certain local direction, where "mod" denotes remainder calculation. The third parameter is feature search length. We believe that stitching task will only require the partial region of image to compare the similarity and it is no need to calculate all information in two images. Therefore, feature search length is the key parameter to control feature search region. It will be initialized as relative small value (for example, 20% of the corresponding edge) and expanded if the algorithm cannot find correct result. By the way, if the feature search length beyond the 50% of the corresponding edge and the algorithm does not find correct stitch, we will assume that these two sequential images cannot be stitched.

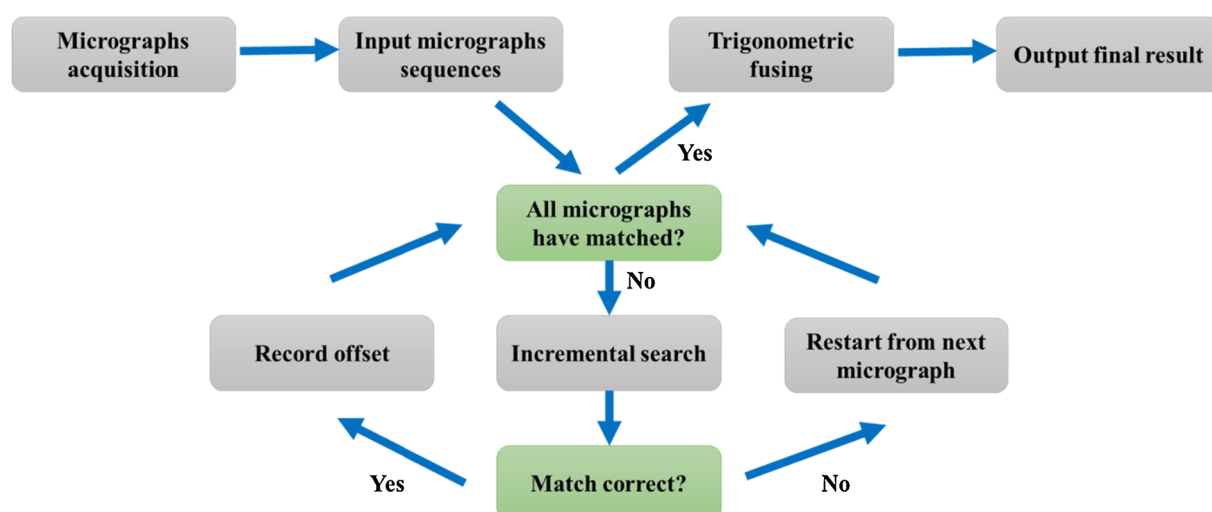


Fig. 3. The flowchart of the VFSMS.

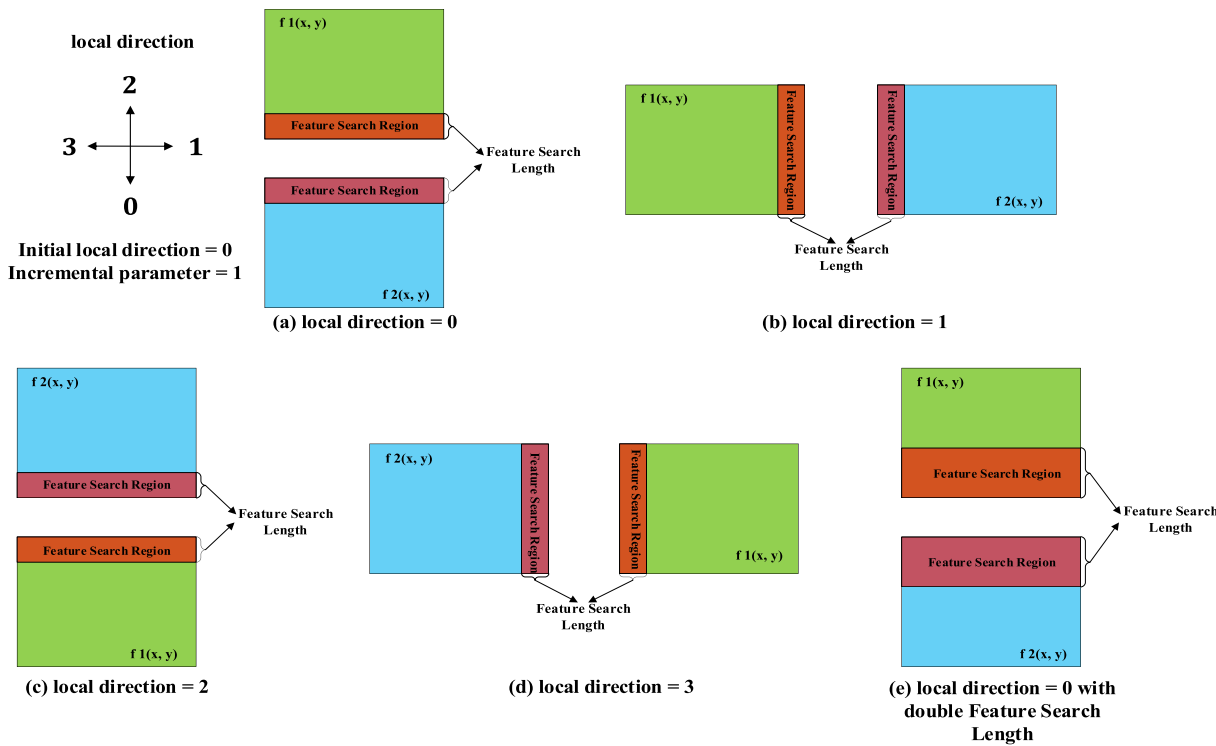


Fig. 4. Diagram of incremental stitching strategy. (a)–(e) shows the updating process of stitching direction by using local direction and incremental parameter. In this example, initial local direction equals 0 and incremental parameter equals 1.

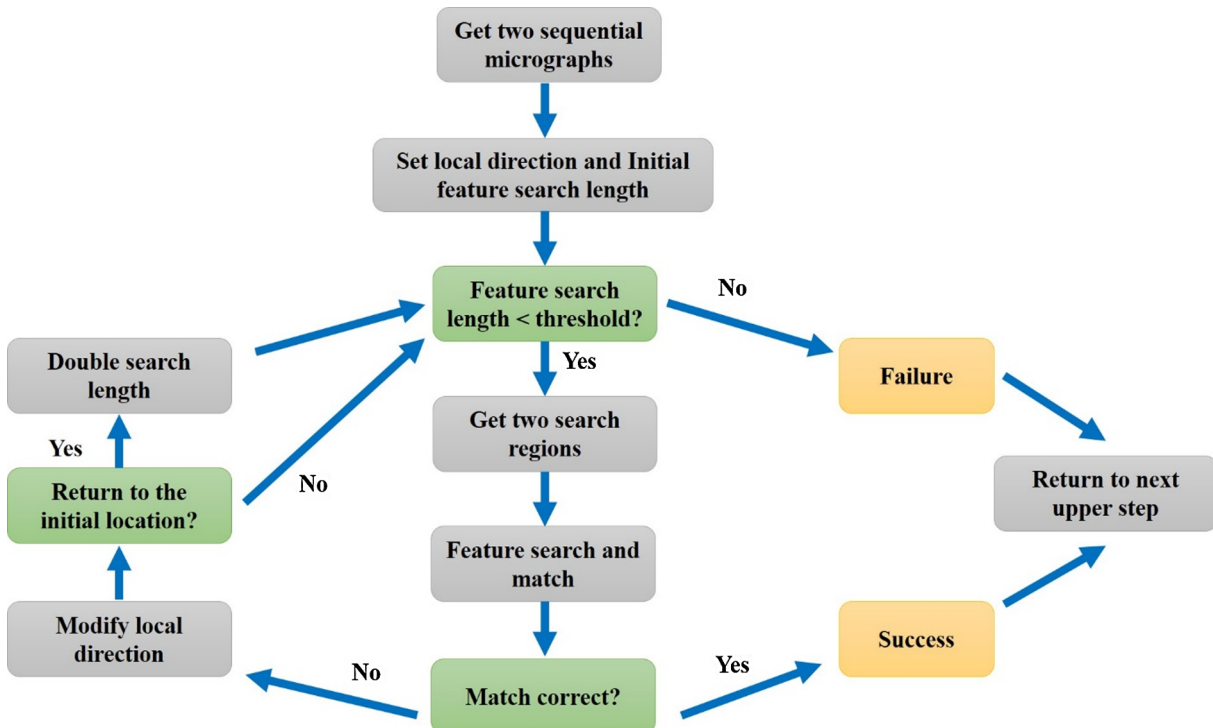


Fig. 5. Flowchart of incremental stitching strategy.

$$\text{local_direction}_{\text{next}} = (\text{local_direction}_{\text{previous}} + \text{Incremental_parameter}) \bmod 4 \quad (1)$$

We will show the procedure of incremental strategy step by step using the Figs. 4 and the 5. First, the VFSMS sets local direction and incremental parameter or inherits it from last stitch (In the Fig. 4, the local direction equals 0 and incremental parameter equals 1). Second, it

initializes feature search length (20% of the corresponding edge in this paper's experiments). Third it stitches images if feature search length is below the certain threshold (50% of the corresponding edge). Fourth, it uses two search regions in corresponding areas of two sequential images, which represented by red translucent regions in the Fig. 4, to find feature points and match them. If match correct, it records the offset and goes back to other processes in the Fig. 3. Otherwise, it

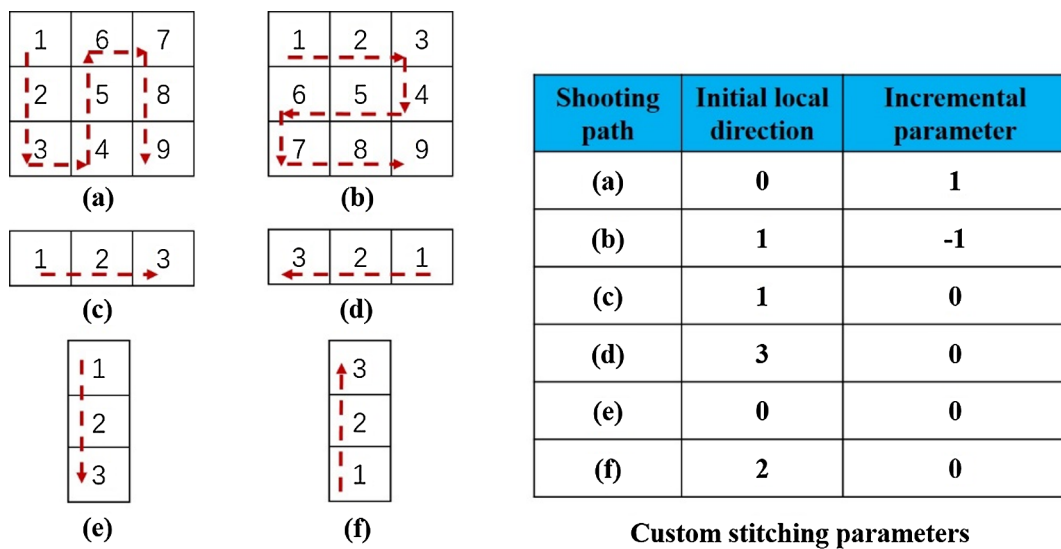


Fig. 6. Custom stitching parameters according to shooting path.

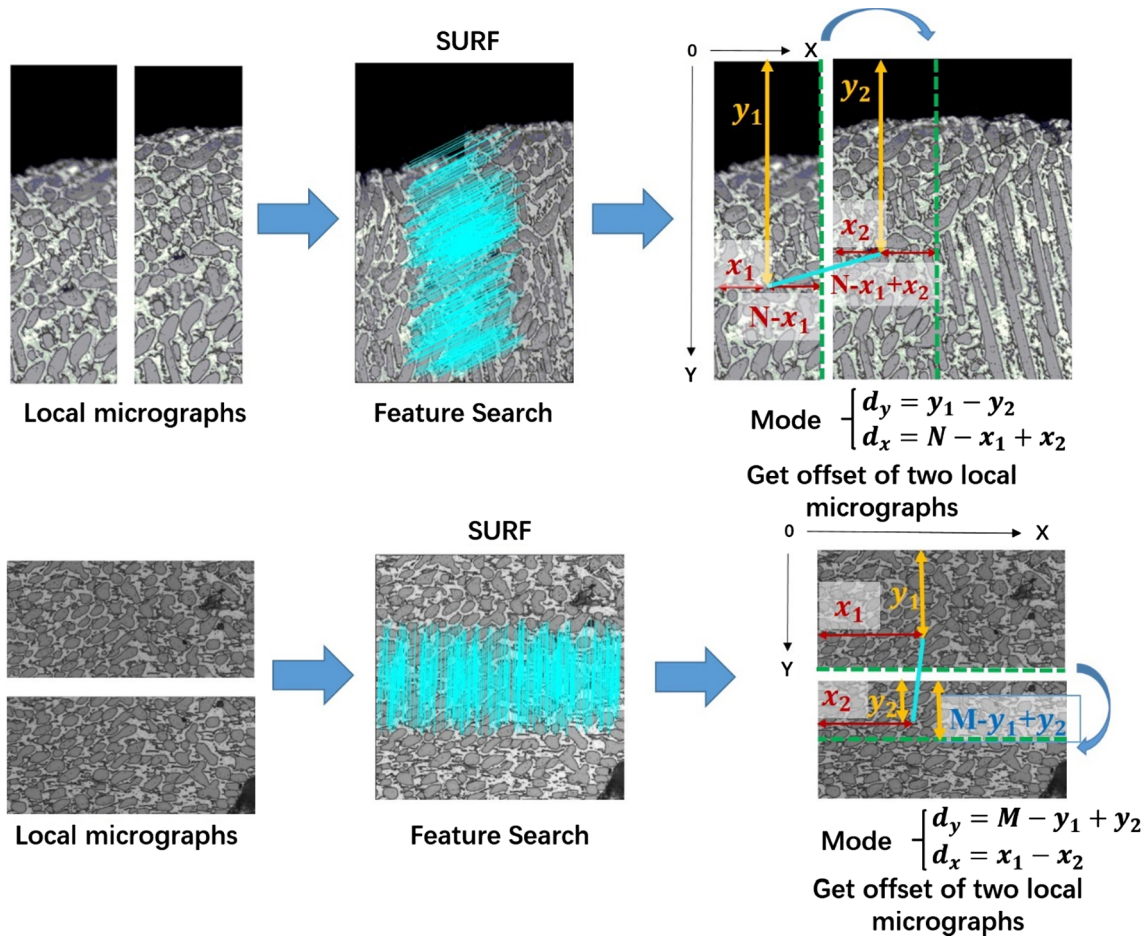


Fig. 7. Matching strategy for two sequential micrographs. M, N denote the rows and columns of the micrograph.

modifies the local direction by using above Eq. (1), for example, from the Fig. 4(a)–(d). We can use default value of local direction and incremental parameter to let algorithm to find correct stitching result (local direction equals 0, and incremental parameter equals 1). In addition, we can customize these parameters to let the algorithm change the direction of feature search length increment, according to different shooting paths (see Fig. 6). For example, if the image is taken from right

to left, the initial local direction can be set to 3, and the incremental parameter can be set to 0. Therefore, the algorithm can accelerate the stitching speed by customizing key parameters to decrease the number of searching, according to different shooting paths. Fifth, we double the search length in order to access more micrographs information and carry the loop if it returns to the initial direction, as shown in the Fig. 4(e). Finally, it will record the offset if match correct. Otherwise, it

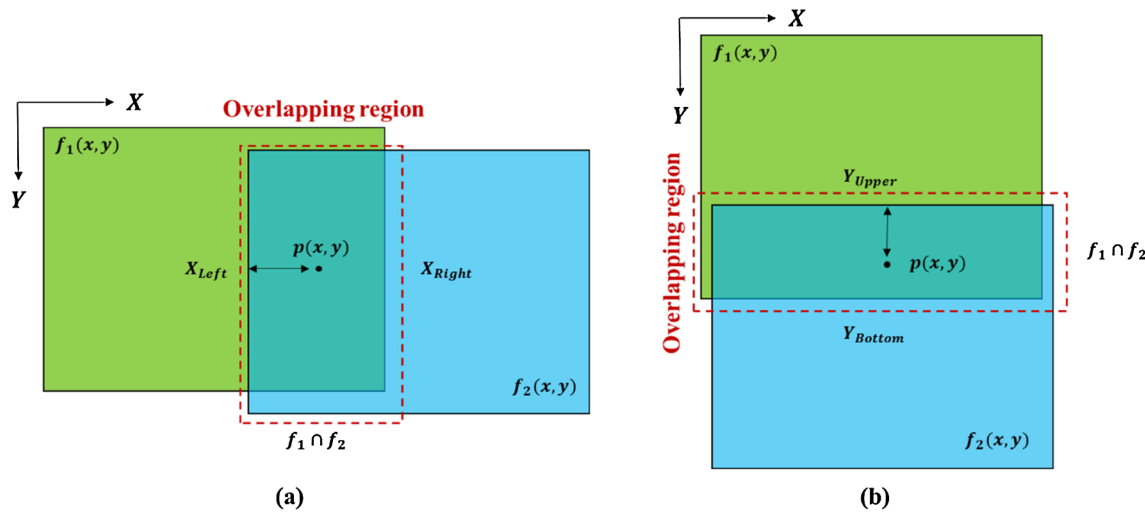


Fig. 8. Fusing demonstration. (a) left-right pairwise image fusion. (b) upper-bottom pairwise image fusion.

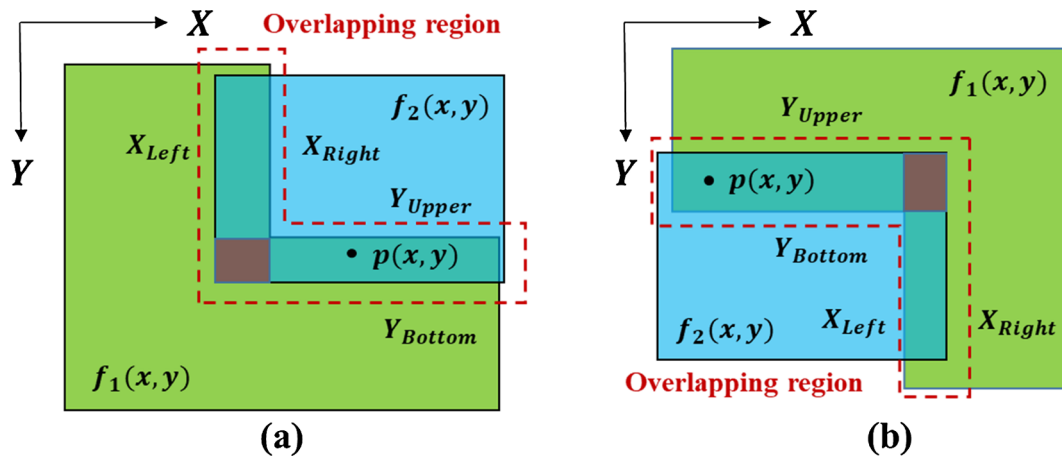


Fig. 9. ‘Corner’ stitching fusing demonstration. (a) left-bottom corner. (b) right-upper corner. The red translucent region denotes corner region. (For interpretation of the references to color in this figure legend, the reader is referred to the web version of this article.)

will report to the algorithm that these two sequential images cannot be stitched.

By using incremental searching strategy, the algorithm needs only partial of images to calculate the offset. Therefore, it will save the consumption of resources and increase the speed of the stitching task.

To realize the stitching of microscopic images with high speed and high accuracy, SURF algorithm [10] was chosen to extract image features in this paper. It has been proved to have a good performance than SIFT and ORB. Besides, the speed of searching feature points would have notable enhancement because of GPU acceleration.

2.3. Matching

Incremental searching strategy needs algorithm to detect the mismatch in order to transform to the next direction. However, traditional matching strategies of feature based methods such as homography and ransac cannot detect the mismatch effectively. Besides, phase correlation based methods just only pick the first peak value in correlation plane of image, which also cannot detect the mismatch.

Therefore, we build a matching method that is suited to incremental searching strategy. We assume all transformations between overlapping images to be translation only which is reasonable for most commonly used microscopy techniques where the static, fixed sample rests on a level microscope slide moved by a motorized stage. The matching strategies are shown in the Fig. 7.

In the Fig. 7, the first row represents horizontal stitching. The second row represents vertical stitching. The green¹ line denotes the location of border of the first micrograph actually correspond to the location in the second micrograph. The blue line denotes a pair of registered surf feature points. SURF is a feature search algorithm, and it can extract many pairs of feature in the two sequential micrographs. In addition, we use ratio of closest to second-closest neighbors [8] of each key-point to register pair of key-points. For our stitching experiment, we reject all matches in which the distance ratio is greater than 0.75. For each pair, we can calculate the offset ('dy' and 'dx') according to the location of two points. Finally, we could get the mode of offsets, which is the value that appears most often in data set. In addition, if the number of mode value beyond a threshold (in our experiment, we set 3), we can convince that the offset is correct.

2.4. Image fusion

There are overlapping areas in the stitching process, as described in the Figs. 8 and 9. Due to imaging principle of microscope, the border of micrograph will have lower luminance than the center region, which will cause obvious seamline in stitching result, as shown in Fig. 10.

We use trigonometric functions [30] to fuse two overlapping regions

¹ For interpretation of color in Fig. 7, the reader is referred to the web version of this article.

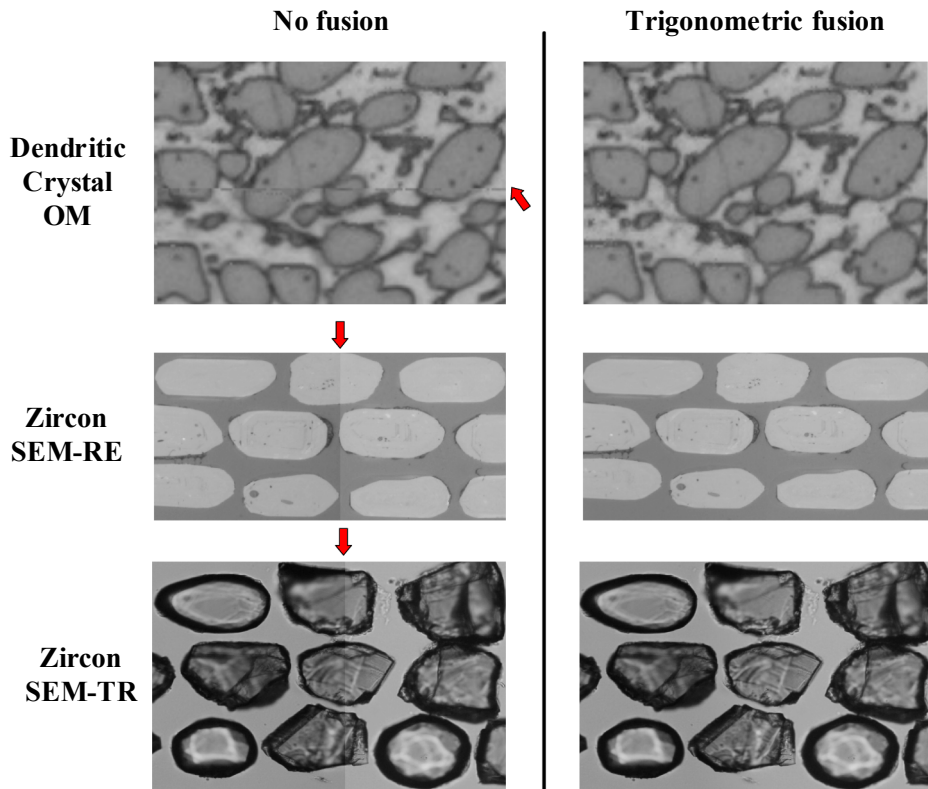


Fig. 10. Fusing results. The first column represents stitching without fusing operation. The second column represents stitching with trigonometric fusing operation. The red arrows denote obvious seamlines. (For interpretation of the references to color in this figure legend, the reader is referred to the web version of this article.)

Table 1
Images datasets.

Types Dimensions (pixel × pixel)	Dendritic Crystal OM (1936 × 2584)	Iron Polycrystal OM (1936 × 2584)	Zircon SEM-BS (1024 × 1280)	Zircon SEM-CL (1024 × 1280)	Zircon SEM-RE (1728 × 2592)	Zircon SEM-TR (1728 × 2592)
Group	1	90	2	4	24	11
	2	90	2	6	20	12
	3	90	2	27	20	13
	4	90	2	25	23	9
	5	91	2	22	24	14
	6	90	2	28	23	10
	7	91	2	30	24	8
	8	90	2	22	21	14
	9	90	2	24	16	12
	10	90	2	24	18	9

in order to eliminate seamline. Let $f_1(x, y)$ and $f_2(x, y)$ represent the two sequential local micrographs, $f(x, y)$ denotes the fusing result, each pixel value can be given by the following equation:

$$f(x, y) = \begin{cases} f_1(x, y), & x, y \in f_1 \\ w_1f_1(x, y) + w_2f_2(x, y), & x, y \in (f_1 \cap f_2) \\ f_2(x, y), & x, y \in f_2 \end{cases} \quad (2)$$

where

$$w_1 = \cos^2\left(\frac{\pi*(x - x_{left})}{2*(x_{right} - x_{left})}\right), \quad w_2 = \sin^2\left(\frac{\pi*(x_{right} - x)}{2*(x_{right} - x_{left})}\right) \text{ or}$$

$$w_1 = \cos^2\left(\frac{\pi*(Y - Y_{upper})}{2*(Y_{bottom} - Y_{upper})}\right), \quad w_2 = \sin^2\left(\frac{\pi*(Y_{bottom} - Y)}{2*(Y_{bottom} - Y_{upper})}\right)$$

where Y_{upper} , Y_{bottom} , X_{right} , X_{left} denote the upper edge, lower edge, right edge and left edge of overlapping region of the two images respectively (see the Fig. 8). w_1 and w_2 are weighting parameters which control fusion result of two pixel value.

However, this method is designed to fuse pairwise micrographs. We make an improvement according to sequential stitching strategy especially for the ‘corner’ stitching (see the Fig. 9). The equation of corner region stitching is:

$$f(x, y) = \begin{cases} f_1(x, y), & x, y \in f_1 \\ w_1f_1(x, y) + w_2f_2(x, y), & x, y \in l - r \text{ region} \\ w_3f_1(x, y) + w_4f_2(x, y), & x, y \in u - b \text{ region} \\ w_1w_3f_1(x, y) + (1 - w_1w_3)f_2(x, y), & x, y \in c \text{ region} \\ f_2(x, y), & x, y \in f_2 \end{cases} \quad (3)$$

where w_3 and w_4 are calculated as same as pairwise stitching. l means left, r means right, u means upper, b means bottom, c means corner.

Some examples of fusing results are showing in the Fig. 10. As shown in the figure, trigonometric image fusion can eliminate obvious seamline perfectly.

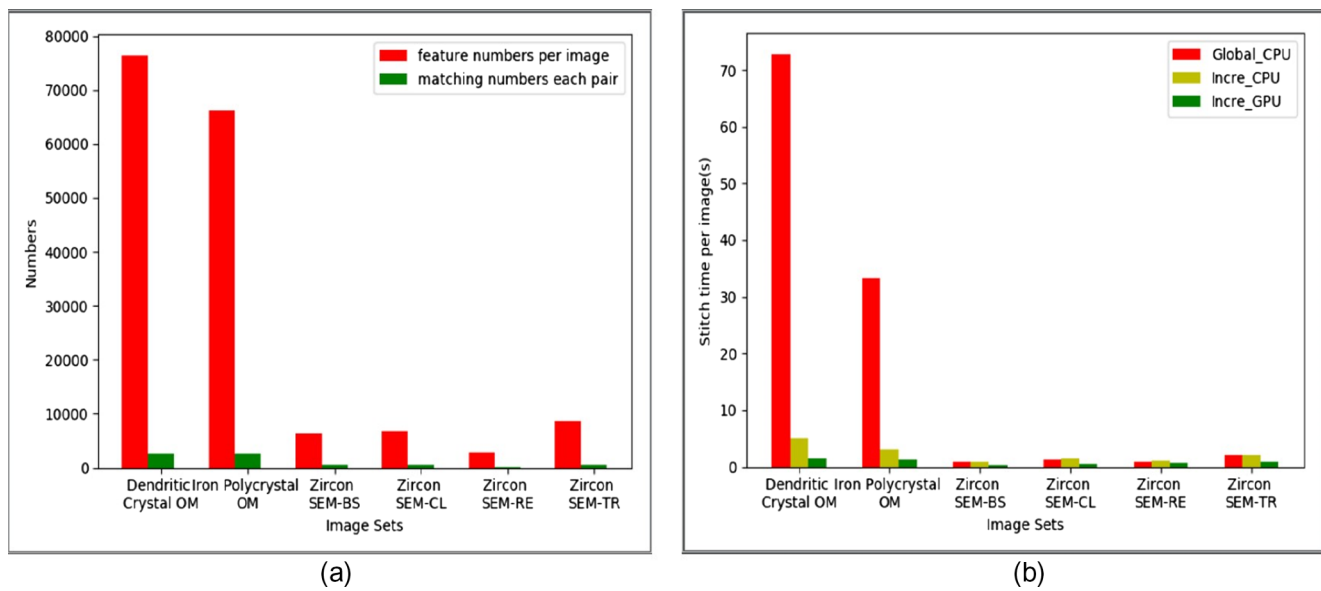


Fig. 11. Time consumption with different methods.

Table 2

Time per image of VFSMS and other software (* is stitching mode in Image-J, the unit is second).

Types	Dendritic crystal OM	Iron polycrystal OM	Zircon SEM-BS	Zircon SEM-CL	Zircon SEM-RE	Zircon SEM-TR	Average
VFSMS	1.55	0.75	0.36	0.35	0.63	1.00	0.77
Grid Stitch*	2.10	1.99	0.30	0.27	1.28	1.30	1.21
Sequential Stitch*	2.78	3.15	0.65	0.41	2.30	2.13	1.90
Pairwise Stitch*	/	2.57	/	/	/	/	/
Photoshop photomerge	3.43	3.56	3.92	5.63	2.46	3.75	3.79
AutoStitch	0.65	2.08	0.55	0.35	0.83	3.32	1.30

Table 3

Accuracy of VFSMS and other software (* is stitching mode in Image-J).

Types	Dendritic crystal OM	Iron polycrystal OM	Zircon SEM-BS	Zircon SEM-CL	Zircon SEM-RE	Zircon SEM-TR	Average
VFSMS	100%	100%	100%	100%	100%	100%	100%
Grid Stitch*	50%	100%	60%	100%	100%	100%	73%
Sequential Stitch*	0%	100%	100%	0%	30%	100%	55%
Pairwise Stitch*	/	100%	/	/	/	/	/
Photoshop photomerge	40%	100%	0%	0%	0%	20%	27%
AutoStitch	0%	0%	60%	0%	20%	70%	25%

3. Experimental results

3.1. Datasets

As shown in the Fig. 2, we chose three types' micrographs of different materials, different structure and different imaging modes as datasets. Type 1 micrograph is optical microscopy (OM) image of pure iron polycrystalline structure (Iron Polycrystal OM), which as a sample for polycrystalline grain structure. Type 2 micrograph is OM image of dendritic crystalline structure of Al-La alloy (Dendritic Crystal OM), which as a sample for fractal structure. Type 3 micrograph is scanning electron micrographs of zircon block embedded in resin matrix in reflected mode (SEM-RE), transmission mode (SEM-TR), black scattered mode (SEM-BS), and cathodoluminescence mode (SEM-CL) as the samples for two phase/composition structure. Type 1 and type 2 micrographs are provided by Beijing advanced innovation center for materials genome engineering, and type 3 are provided by hebei bureau of geo-information. Type 1 and type 2 micrographs have thousands detailed highly complex and diverse tiny microstructures with different sizes and shapes which increase demand for effectiveness and efficiency

of method. Scientists need image stitching method to observe and analysis large scale of microstructures with high resolution. Type 3 micrographs have a little zircon block in one local image, however, the texture of zircon is very similar which increase demand for robustness of method. Inspectors need large scale of sample to measure geological age. Each type has different dimensions (image sizes, the unit is pixel). Each type has ten groups of sub-image datasets for parallel tests to ensure the reliability of experimental results. Each group has different numbers of micrographs according to the shooting situation as shown in Table 1. All the local micrographs in each group can be stitched to form a global composite one. In total, we have 1584 micrographs for stitching performance testing.

3.2. Implementation and evaluation details

Our implementation of VFSMS was derived from the publicly available python [31], numpy [32] and opencv toolbox [33]. In addition, all the experiments are conducted on an E5-2687W Intel core of a 2.60 GHz Windows workstation with 16 GB of memory and Nvidia Quadro K1200 with a graphics memory of 4 GB [34].

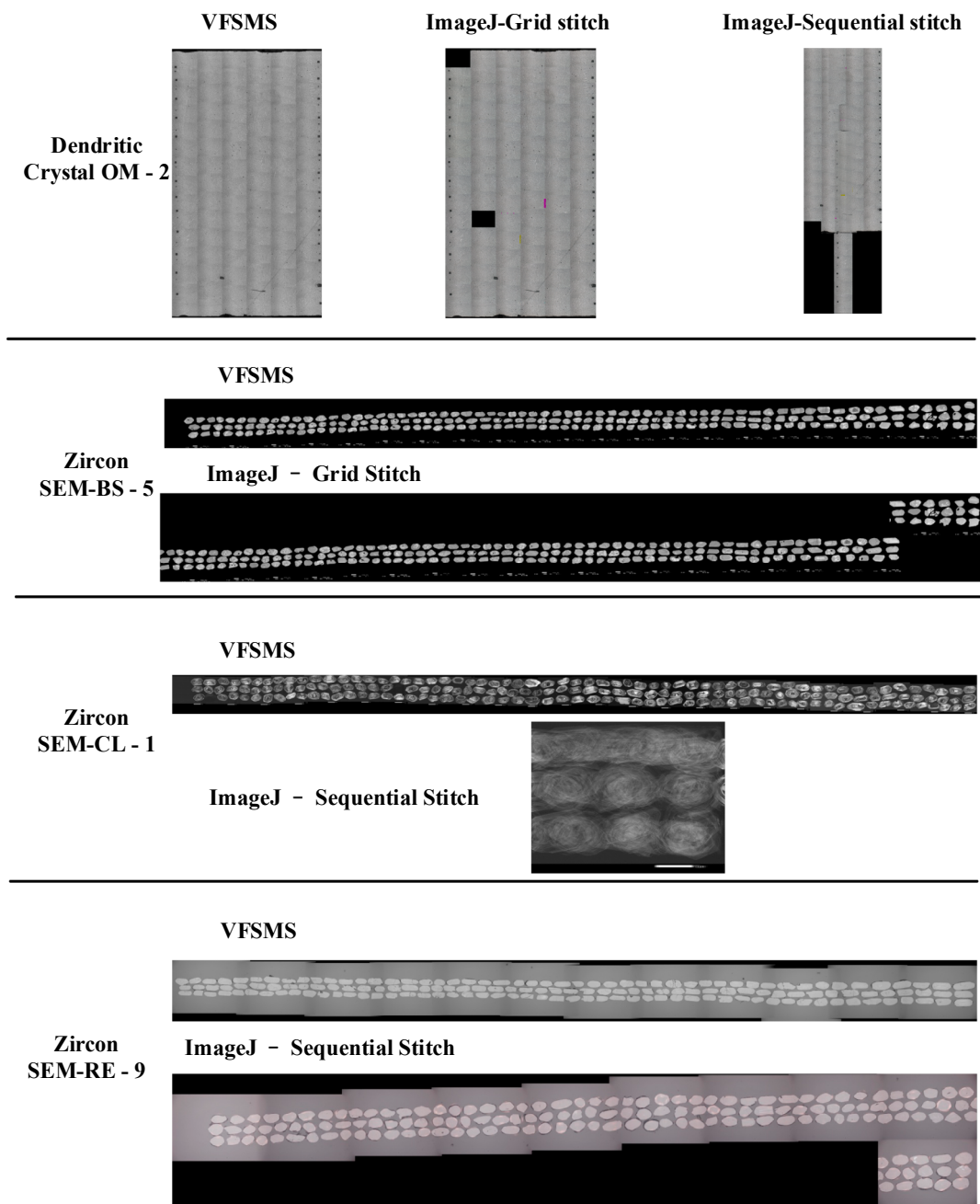


Fig. 12. Some examples of VFSMS and ImageJ.

In this work, we use the accuracy and time consumption to evaluate performance of stitching strategy and software. The accuracy in each type was calculated as following formula and it was evaluated by material scientists. In experiments, they judged whether the stitching was correct by observing whether there was a misplacement which can tell by human eyes on both sides of the stitching line.

$$\text{Accuracy}_T = \frac{N_{right}}{N_{total}} \times 100\% \quad (4)$$

where N_{right} means the number of groups which stitching result have no observably misplacement, N_{total} means total groups in type T.

3.3. Time consumption for feature search in VFSMS

Feature based stitching would have high accuracy, but it will cost a lot of time consumption if there are thousands of feature points in local

micrographs. For micrographs of dendritic crystal and iron polycrystal in particular, those microstructures are always highly complicated. That will cause much more time consumption shown in Fig. 11. As shown in the Fig. 11(a), we demonstrate feature numbers and matching numbers per image in the three types' datasets. Dendritic crystal and iron polycrystal images have nearly same dimensions compared to other datasets, however, the feature numbers of those are eight times larger than the other's. Therefore, the time consumption of those is thirty-six times larger than the other's in CPU mode as shown in the Fig. 11(b).

Incremental searching strategy is a highly effectively method which suites for feature based and sequential stitching. In the Fig. 11(b), incremental strategy is much faster than the method without it, even in the CPU mode. Besides, GPU acceleration can further improve the speed of stitching especially for the dendritic and iron polycrystal which have thousands of features. However, GPU acceleration would have little

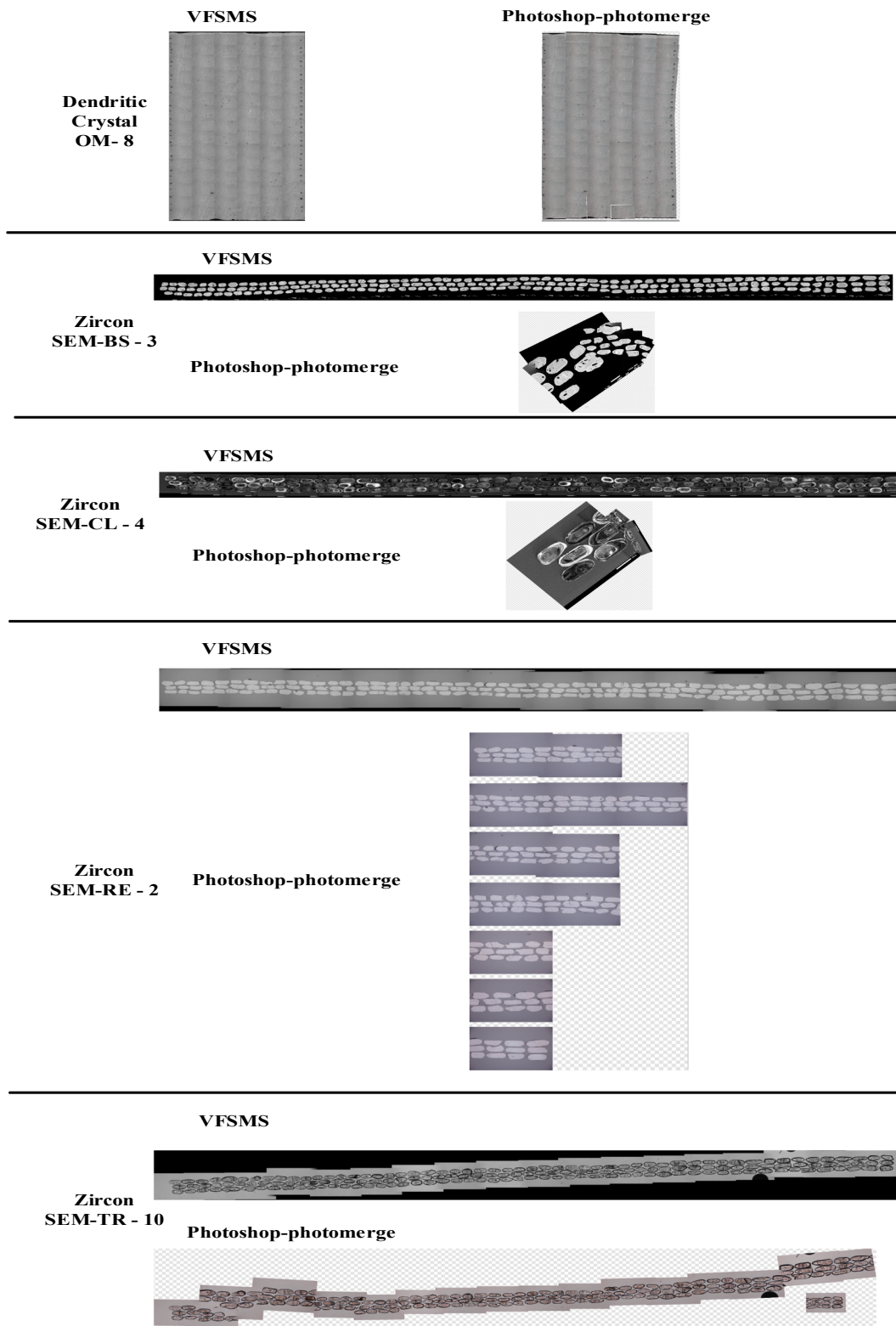


Fig. 13. Some examples of VFSMS and Photoshop.

influence when applied to the certain datasets which have lower feature points. That is because that there is some inevitable time consumption spends on data migration from CPU to GPU.

3.4. Performance evaluation

We compare the performance of VFSMS with other software, such as

ImageJ (1.51 s) [21,22], Photoshop-photomerge [23,24] and Autostitch [17,28]. There are three types of stitching strategies in ImageJ (1.51 s): grid stitch, sequential stitch and pairwise stitch. Grid stitch needs user to specify the size of grid and shooting path in order to increase accuracy of stitching and decrease time consumption by using multi-threaded CPU programing [27]. Sequential stitch do not need to design the shooting path as same as VFSMS. Pairwise stitch can only stitch two

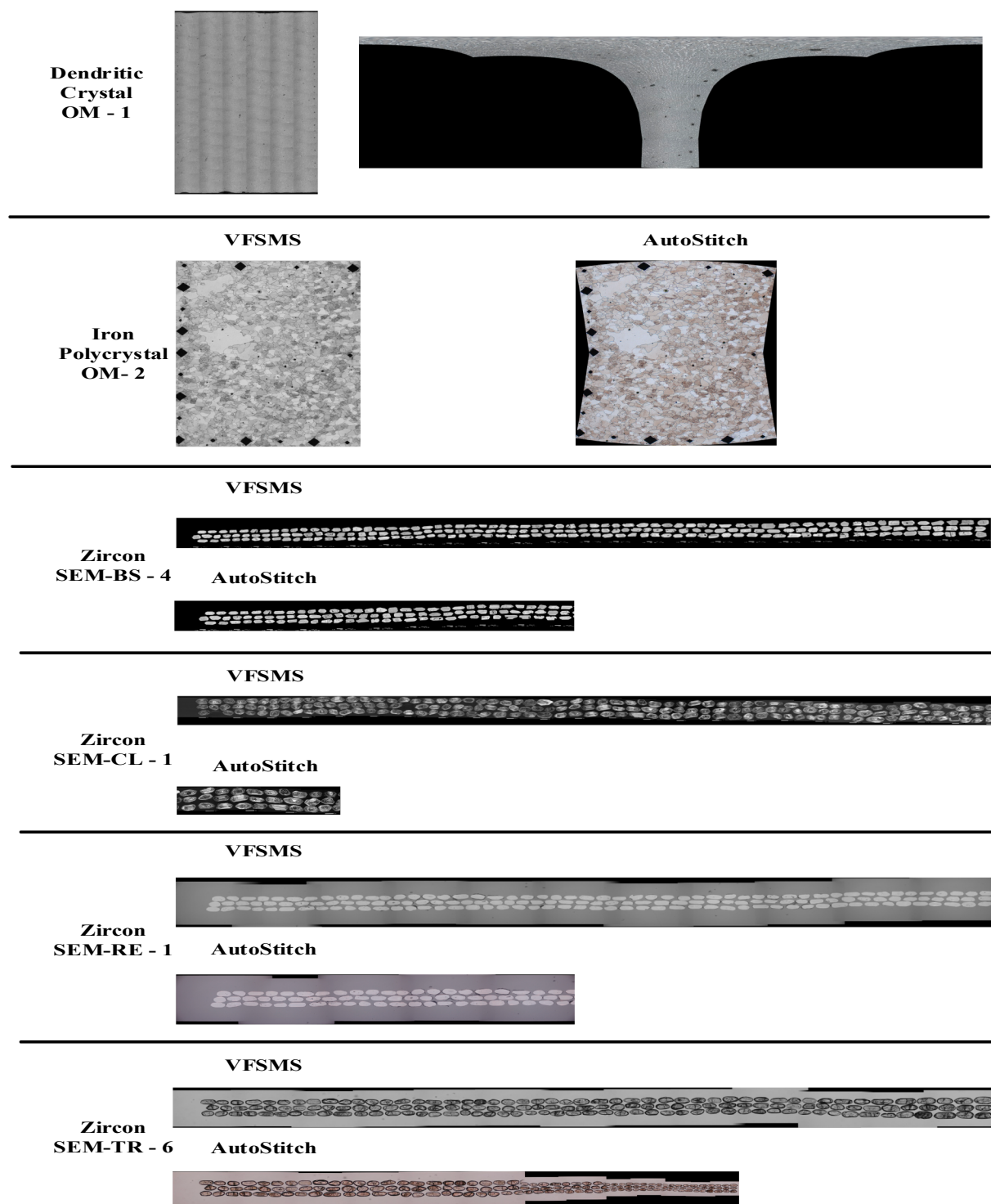


Fig. 14. Some examples of VFSMS and Autostitch.

sequential micrographs which are not suited to large numbers of local micrographs. For Photoshop, we use collage mode in photomerge plugin. In addition, ImageJ and Photoshop use phase correlation based stitching strategy. While Autostitch use feature based stitching strategy. All experiments are implemented on the machine that has described in the [Section 3.2](#).

We compare the performance of VFSMS and other software in [Tables 2](#) and [3](#). We calculate the average time consumption per image and statistic the accuracy of the images for each type in different methods. For dendritic crystal micrographs, Autostitch would omit

some micrographs that it cannot match, so that the duration of calculation time is very small, however, the accuracy of stitching result is zero. For zircon SEM-CL and zircon SEM-BS datasets, the VFSMS would be a little slower than the ImageJ with grid mode, that is because there is some duration time wasted in the data transformation between CPU and GPU. However, the VFSMS is more robust than ImageJ in the accuracy aspect. Some examples are shown in the [Fig. 12](#).

There are three types of micrographs with 1584 micrographs in total. Each type of micrograph has ten groups of sub image data and each group have a series of images which could be stitched to a global

one. Therefore, we refer one group of images stitching task as one test and there are 60 tests in total. However, the assessment is a very strict standard. It means the result would be correct only if the stitching result of all micrographs in one group has no observably misplacement. According to the accuracy assessment method described in [Section 3.2](#), the denominator N_{total} is always 10. And the numerator N_{right} is range from 0 to 10.

Experimental results demonstrate that VFSMS achieves state-of-art performance on several microscopic datasets on both accuracy and speed aspects. Besides, it significantly outperforms the most famous and commonly used software, such as ImageJ, Photoshop and Autostitch. The average time consumption of VFSMS is 60% of ImageJ, which is most popular software in material image processing. In addition, VFSMS achieves 100% accuracy in experimental datasets, which is more robust than other software.

4. Analysis and comparison

We demonstrate some examples of stitching results of VFSMS and other software in this section.

In the [Fig. 12](#), we show some stitching results of VFSMS and ImageJ (1.51 s). Each row refers to one sample. ‘Dendritic crystal OM-2’ represents the second group in dendritic crystal OM dataset. As described in the [Section 3.4](#), there are grid, sequential and pairwise mode in ImageJ. Grid stitch needs user to specify the shooting path and grid size. It can eliminate accumulative error so that error in one line would not influence the other line, as shown in the second image of the first row. Moreover, ImageJ is a phase correlation based software. It may yield ambiguous results when micrographs contain much of similar microstructures [[26](#)]. Besides, ImageJ doesn’t split the mismatch result which causes troubles for users, shown in the dendritic crystal OM-2, Zircon SEM-BS-5, Zircon SEM-CL-1 and Zircon SEM-RE-9 samples.

In [Fig. 13](#), we show some stitching results of VFSMS and Photoshop. For fairly comparison, we use collage mode in photomerge plugin. As same as ImageJ, Photoshop is a phase correlation based software. In addition, it picks up an improved version which can detect rotation of image. However, for most microscopic research, we commonly use microscope equipped with motorized stage, which will not cause rotation in sequential micrographs. Unfortunately, it also yields ambiguous results when micrographs contain much of similar microstructures.

In [Fig. 14](#), we show some stitching results of VFSMS and AutoStitch. AutoStitch is a feature based software. It is particularly suited to stitch images in nature scene and doesn’t have good results in micrograph stitching. It employ SIFT, ransac and homography strategy which can detect projective transformation in sequential images. However, those methods can cause large deformation when applied to micrograph stitching, as shown in dendritic crystal OM-1, iron polycrystal OM-2 and zircon SEM-TR-6 samples. Besides, Autostitch will abort stitch when it detect mismatch, which is not suited to scientific research. By contrast, VFSMS will save previous stitching result and restart the stitch on the next images when it faces mismatch.

5. Conclusion

In this work, in order to handle the task of micrograph stitching, we develop a very fast sequential micrograph stitching method, named VFSMS, which employ incremental searching strategy and GPU acceleration to guarantee the accuracy and speed of the stitching results. By using those strategies, we can stitch several local images with overlapping areas to form a final global composite one with huge resolution. Experimental results demonstrate that VFSMS achieves state-of-art performance on three types’ microscopic datasets on both accuracy and speed aspects. Besides, it significantly outperforms the most famous and commonly used software, such as ImageJ, Photoshop and Autostitch.

The limitation of VFSMS is that it only fuses local micrographs in gray mode and doesn’t fuse micrographs in RGB channels, which will

lose color information in micrographs. Besides, there is little tiny distortion in the dendritic crystal’s stitching result which might be caused by imaging principle of microscope. Our team will work on this problem in subsequent work.

CRediT authorship contribution statement

Boyuan Ma: Methodology, Writing - original draft. **Xiaojuan Ban:** Conceptualization. **Haiyou Huang:** Conceptualization. **Wanbo Liu:** Data curation. **Chuni Liu:** Validation. **Di Wu:** Writing - review & editing. **Yonghong Zhi:** Writing - review & editing.

Acknowledgements

The authors acknowledge the financial support from the National Key Research and Development Program of China (No. 2016YFB0700500), and the National Science Foundation of China (No. 61572075, No. 61702036, No. 51574027), and Fundamental Research Funds for the Central Universities (No. FRF-TP-17-012A1), and China Postdoctoral Science Foundation (No. 2017M620619). Besides, we gratefully thanks to Dr. Siliang He and Prof. Qiang Feng for providing Fig. 1 for illustration.

Appendix A. Supplementary material

Supplementary data to this article can be found online at <https://doi.org/10.1016/j.commatsci.2018.10.044>.

References

- [1] ASM handbook: metallography and microstructures, ASM International, 1985.
- [2] L. Duval, M. Moreaud, C. Couprise, et al., Image processing for materials characterization: issues, challenges and opportunities, 2014 IEEE International Conference on, Image Processing (ICIP), IEEE, 2014, pp. 4862–4866.
- [3] J. Hu, Y.N. Shi, X. Sauvage, et al., Grain boundary stability governs hardening and softening in extremely fine nanograined metals, *Science* 355 (6331) (2017) 1292–1296.
- [4] Q. Wu, F. Merchant, K. Castleman, *Microscope Image Processing*, Academic press, 2010.
- [5] M. Sonka, V. Hlavac, R. Boyle, *Image Processing, Analysis, and Machine Vision*, Cengage Learning, 2014.
- [6] F. Yang, Z.S. Deng, Q.H. Fan, A method for fast automated microscope image stitching, *Micron* 48 (2013) 17–25.
- [7] E. Adel, M. Elmogy, H. Elbakry, Image stitching based on feature extraction techniques: a survey, *Int. J. Comput. Appl.* 0975–8887 (2014).
- [8] D.G. Lowe, Distinctive image features from scale-invariant keypoints, *Int. J. Comput. Vision* 60 (2) (2004) 91–110.
- [9] A.A. Fathima, R. Karthik, V. Vaidehi, Image stitching with combined moment invariants and sift features, *Procedia Computer Science* 19 (2013) 420–427.
- [10] H. Bay, T. Tuytelaars, L. Van Gool, Surf: speeded up robust features, European Conference on Computer Vision, Springer, Berlin, Heidelberg, 2006, pp. 404–417.
- [11] L. Juan, G. Oubong, SURF applied in panorama image stitching, 2010 2nd International Conference on Image Processing Theory Tools and Applications (IPTA), IEEE, 2010, pp. 495–499.
- [12] E. Rublee, V. Rabaud, K. Konolige, et al., ORB: An efficient alternative to SIFT or SURF, 2011 IEEE International Conference on Computer Vision (ICCV), IEEE, 2011, pp. 2564–2571.
- [13] Y. Pang, W. Li, Y. Yuan, et al., Fully affine invariant SURF for image matching, *Neurocomputing* 85 (2012) 6–10.
- [14] Y. Ruiyang, Research of Medical Microscopic Image Mosaic Based on SURF Algorithm, Lanzhou University, 2014.
- [15] M.A. Fischler, R.C. Bolles, A paradigm for model fitting with applications to image analysis and automated cartography, *Comm. ACM* 24 (6) (1981) 381–395.
- [16] M. Brown, D.G. Lowe, Recognising panoramas, in: IEEE International Conference on Computer Vision, 2003, 3, pp. 1218.
- [17] M. Brown, D.G. Lowe, Automatic panoramic image stitching using invariant features, *Int. J. Comput. Vision* 74 (1) (2007) 59–73.
- [18] F. Yang, Y. He, Z.S. Deng, et al., Improvement of automated image stitching system for DR X-ray images, *Comput. Biol. Med.* 71 (2016) 108–114.
- [19] B.S. Reddy, B.N. Chatterji, An FFT-based technique for translation, rotation, and scale-invariant image registration, *IEEE Trans. Image Process.* 5 (8) (1996) 1266–1271.
- [20] H. Dogan, M. Ekinci, Automatic panorama with auto-focusing based on image fusion for microscopic imaging system, *Signal, Image Video Process.* 8 (1) (2014) 5–20.
- [21] J. Schindelin, I. Arganda-Carreras, E. Frise, et al., Fiji: an open-source platform for

- biological-image analysis, *Nature methods* 9 (7) (2012) 676.
- [22] ImageJ: Available online: <<https://imagej.nih.gov/ij/index.html>> .
- [23] David Biedny, *The Official Adobe Photoshop Handbook*, Random House Inc., 1991.
- [24] Adobe PhotoShop CC 2018. Available online: <<https://www.adobe.com/products/photoshop.html>> .
- [25] L. Carozza, A. Bevilacqua, F. Piccinini, An incremental method for mosaicing of optical microscope imagery, 2011 IEEE Symposium on Computational Intelligence in Bioinformatics and Computational Biology (CIBCB), IEEE, 2011, pp. 1–6.
- [26] J.N. Sarvaiya, S. Patnaik, K. Kothari, Image registration using log polar transform and phase correlation to recover higher scale, *J. Pattern Recognition Res.* 7 (1) (2012) 90–105.
- [27] S. Preibisch, S. Saalfeld, P. Tomancak, Globally optimal stitching of tiled 3D microscopic image acquisitions, *Bioinformatics* 25 (11) (2009) 1463–1465.
- [28] AutoStitch, Available online: <<http://matthewalunbrown.com/autostitch/autostitch.html>> .
- [29] B. Ma, T. Zimmerman, M. Rohde, et al., Use of Autostitch for automatic stitching of microscope images, *Micron* 38 (5) (2007) 492–499.
- [30] W. Dan, L. Hui, L. Ke, An image fusion algorithm based on trigonometric functions, *Infrared Technol.* 39 (1) (2017) 53–57.
- [31] Python Software Foundation: Python language reference. <http://www.python.org>.
- [32] Numpy. Available online: <http://www.numpy.org/>.
- [33] R. Laganière, *OpenCV 3 Computer Vision Application Programming Cookbook* [M], Packt Publishing Ltd, 2017.
- [34] Quadro K1200. Available online: <http://images.nvidia.com/content/quadro/product-literature/data-sheets/11306_DS_NV_Quadro_K1200_FEB15_NV_US_HR.pdf> .